Frequency of Coronary Microvascular Dysfunction and Diffuse Myocardial Fibrosis (Measured by Cardiovascular Magnetic Resonance) in Patients With Heart Failure and Preserved Left Ventricular Ejection Fraction

Adrián I. Löffler, MD[a], Jonathan A. Pan, MD[a], Pelbreton C. Balfour, Jr.MD, ScM[a], Peter W. Shaw, MD[a], Yang Yang, PhD[b], Moiz Nasir, BS[a], Daniel A. Auger, PhD[a,b], Frederick H. Epstein, PhD[a,b], Christopher M. Kramer, MD[a,c], Li-Ming Gan, MD[d,e], and Michael Salerno, MD, PhD, MS[a,b,c,*]

Heart failure with preserved ejection fraction (HFpEF) is frequently accompanied by co-morbidities and a systemic proinflammatory state, resulting in coronary microvascular dysfunction (CMD), as well as myocardial fibrosis. The purpose of this study is to examine the relation between myocardial perfusion reserve (MPR) and diffuse myocardial fibrosis in patients with HFpEF using cardiovascular magnetic resonance. A single center study was performed in 19 patients with clinical HFpEF and 15 healthy control subjects who underwent quantitative first-pass perfusion imaging to calculate global MPR. T1 mapping was used to assess fibrosis and to calculate extracellular volume. Spiral cine displacement encoded stimulated echo was used to calculate myocardial strain. Comprehensive 2D echocardiograms with speckle tracking, cardiopulmonary exercise testing, and brain natriuretic peptide levels were also obtained. In patients with HFpEF, mean left ventricular EF was 61% ± 9% and left ventricular mass index 45 ± 12 g/m^2. Compared with controls, HFpEF patients had reduced global MPR (2.29 ± 0.64 vs 3.38 ± 0.76, p = 0.002) and VO_2 max (16.5 ± 6.8 vs 30.9 ± 7.7 ml/kg min, p <0.001) whereas extracellular volume (0.29 ± 0.04 vs 0.25 ± 0.04, p = 0.02), pulmonary artery systolic pressure (35.4 ± 13.7 vs 22.3 ± 5.4 mm Hg, p = 0.004), and average E/e' (15.0 ± 7.6 vs 8.6 ± 2.0, p = 0.005) were increased. Displacement encoded stimulated echo peak systolic circumferential strain (p = 0.60) as well as echocardiographic derived global longitudinal strain (p = 0.07) were similar between both groups. The prevalence of CMD, defined as global MPR <2.5, in the HFpEF group was 69%. In conclusion, HFpEF patients have a high prevalence of CMD and diffuse fibrosis. These parameters may be useful clinical end points for future therapeutic trials. **(Am J Cardiol 2019;124:1584−1589)**

Background

Heart failure (HF) with preserved ejection (HFpEF) is frequently accompanied by systemic co-morbidities.[1,2] Inflammation affects the coronary microvascular endothelium which results in vasoconstriction in HFpEF patients.[2] Coronary microvascular dysfunction (CMD), assessed invasively,[3,4] noninvasively,[5,6] and on autopsy[7] may be involved in the pathogenesis of HFpEF. CMD assessment by quantitative stress perfusion cardiovascular magnetic resonance (CMR) has not been previously studied in HFpEF. Myocardial perfusion reserve (MPR) by CMR has been validated against invasive[8] and noninvasive modalities (positron-emission tomography [PET]).[9] CMR can also quantify diffuse myocardial fibrosis which is a common end point of many cellular processes in HFpEF patients.[7,10] T1 mapping post-gadolinium and quantification of extracellular volume fraction (ECV) by CMR has been shown to be markers of diffuse myocardial fibrosis.[11−15] We hypothesized that patients with HFpEF will have reduced global MPR and increased ECV compared with age-matched controls and that these indices would be associated with echocardiographic evidence of diastolic dysfunction, exercise capacity, and peak VO_2.

Methods

Between May 2015 and November 2018, patients with a confirmed clinical diagnosis of HFpEF were prospectively enrolled in this single center study. This study was performed under a locally approved IRB protocol (HSR#

[a]Department of Medicine, Cardiovascular Medicine Division, University of Virginia Health System, Charlottesville, Virginia; [b]Department of Biomedical Engineering, University of Virginia Health System, Charlottesville, Virginia; [c]Department of Radiology and Medical Imaging, University of Virginia Health System, Charlottesville, Virginia; [d]Department of Cardiology, Sahlgrenska University Hospital, Gothenburg, Sweden; and [e]Cardiovascular, Renal and Metabolism IMED Biotech Unit, AstraZeneca Gothenburg, Mölndal, Sweden. Manuscript received May 30, 2019; revised manuscript received and accepted August 6, 2019.

Funding: Drs. Löffler, Balfour, and Shaw were supported by NIH 5T32EB003841. Dr. Salerno was funded by NIH R01 HL131919. This work was funded by the UVA-AstraZeneca Alliance.

See page 1588 for disclosure information.

*Corresponding author: Tel: (434) 243-7325; fax: (434) 982-1998.
E-mail address: MS5PC@hscmail.mcc.virginia.edu (M. Salerno).

0002-9149/
https://doi.org/10.1016/j.amjcard.2019.08.011

17997), and all patients gave written informed consent before enrollment. The following strict criteria were required for study inclusion: age 18 to 85, New York Heart Association functional class ≥ II or BNP ≥150 pg/ml, EF >45%, and at least grade 1 diastolic dysfunction by echo or elevated pulmonary capillary wedge pressure on right heart catheterization. Exclusion criteria were history of known myocardial infarction or coronary artery disease (CAD), severe valvular heart disease, secondary causes of hypertension, infiltrative or hypertrophic cardiomyopathy, pericardial disease, primary pulmonary arterial hypertension, or previously reduced left ventricular (LV) EF with recovery of function. Subjects with contraindications to magnetic resonance imaging such as metallic implants, severe claustrophobia, pacemakers/defibrillators, and estimated GFR <45 ml/min/1.73 m^2 were also excluded. History of persistent atrial fibrillation with heart rate >100 beats/min were excluded due to concern regarding poor image quality. Patients with a contraindication to adenosine or who refused adenosine were excluded from stress myocardial perfusion imaging but were eligible for the remainder of the study, including native and contrast-enhanced T1 mapping. One patient screened for the study was excluded due to presence of previously unknown constrictive pericarditis.

HFpEF patients were compared with 15 age-matched healthy controls that were free of known cardiovascular disease which were prospectively recruited for this study. All subjects underwent a history and physical examination, electrocardiogram, cardiopulmonary exercise testing, comprehensive transthoracic echocardiogram (including strain), blood tests, and CMR.

CMR studies were performed on a 1.5 Tesla scanner (Avanto or Aera, Siemens Healthineers, Erlangen, Germany). Protocol included scout imaging followed by balanced steady-state free precession cine sequences. A short-axis stack of 8 mm thick short axis images with 2 mm gap covered the entire LV. Three long-axis images were obtained (2, 3, and 4-chamber views). A spiral cine displacement encoding with stimulated echoes (DENSE) pulse sequence was used to quantify peak systolic circumferential strain and early diastolic strain rate.[16–18] Base- and mid-ventricular short-axis modified Look-Locker inversion recovery (MOLLI) T1 mapping images, were then obtained before contrast administration, at 5 and 10 minutes after stress perfusion, and at 5, 10, and 15 minutes after rest perfusion imaging.

For stress perfusion assessment, 3 short axis slice locations were imaged per heart beat over a 60 heart beat acquisition during an IV bolus of 0.075 mmol/kg of gadolinium contrast (Magnevist, Bayer Healthcare) injected through power injector at 4 ml/s. Adenosine was infused at 140 μg/kg per minute through a peripheral IV line for 3 to 4 minutes during the stress imaging. Rest perfusion imaging was performed 15 minutes following stress imaging. Quantitative first-pass perfusion imaging was performed using a dual-sequence approach using a vendor-supplied works in progress package. The saturation-recovery gradient echo pulse sequence acquires a low-resolution arterial input function image, and 3 myocardial tissue function images every RR interval. Two proton density weighted images were acquired for the arterial input function and tissue function for correcting surface-coil related intensity inhomogeneity and Bloch simulation modeling was used to convert the signal intensity into gadolinium concentration units as previously described.[19,20]

Late gadolinium enhancement (LGE) images were also obtained 5 minutes after resting perfusion using standard SCMR guideline protocols.[21] Cine CMR images were analyzed by an experienced investigator using QMASS (Medis Medical Imaging Systems, Leiden, the Netherlands). Short-axis cine images were contoured for each short-axis slice, with total LV mass, end-diastolic volume, end-systolic volume, stroke volume, and EF measured.

Perfusion quantification was performed on a pixel-wise basis using the constrained Fermi function deconvolution method implemented in MATLAB (Mathworks, Natick, Massachusetts).[22] Global MPR was calculated as a ratio of the stress perfusion divided by rest perfusion for each subject. T1 quantification was performed using manual segmentation of the myocardium in MATLAB. The partition coefficient of gadolinium, λ, was calculated from the slope of the linear fit of the plot of 1/T1 myocardium versus 1/T1 blood. ECV was calculated as $\lambda \times$ (1-hematrocrit).[23,24] Hematocrit was measured on the day of the CMR study. Peak systolic circumferential strain and early diastolic strain rates were computed offline from DENSE images with a custom MATLAB script using previously described methods.[18,25,26]

All study participants underwent comprehensive 2D with Doppler, tissue Doppler imaging, and speckle tracking using commercially available ultra sound systems (GE Healthcare, Philips Medical Systems). LV function, diastolic function, and global longitudinal strain (GLS) were quantified as recommended by the American Society of Echocardiography/European Association of Cardiovascular Imaging.[27,28] GLS was analyzed using vendor-independent speckle-tracking echocardiographic software (Tomtec 2D Cardiac Performance Analysis, Tom Tec Imaging Systems, Munich, Germany) on optimized (maximized frame rate, minimizing foreshortening) 2-, 3-, and 4-chamber apical view images. If regional tracking was suboptimal in more than 2 myocardial segments in a single view then GLS calculation was not performed.

All exercise tests were performed at our center's cardiopulmonary exercise laboratory. Metabolic measures were determined during a continuous progressive treadmill protocol. VO_2 max was chosen as the highest 1 minute value obtained at volitional exhaustion. Respiratory exchange ratio ≥1.1, Borg Rating of Perceived Exertion >18, and age predicted maximal heart rate were also used as indicators of attaining VO_2 max.

Analysis was performed using SAS, version 9.4 (SAS Institute, Inc. Cary, North Carolina). Continuous normally distributed data are presented as mean ± SD, and were compared using 2-sided *t* tests. Categorical data are presented as N and percentages and compared using chi-square analysis and the Fisher's exact test where appropriate. For all statistics a $p < 0.05$ was considered statistically significant. Pearson test was used to determine the correlation of different covariates with ECV and MPR.

Results

A total of 34 subjects were included in the study, 19 patients with HFpEF and 15 healthy age-matched controls.

Table 1
Baseline characteristic of heart failure with preserved ejection fraction (HFpEF) patients and controls

Variable	HFpEF (n = 19)	Controls (n = 15)	p Value
Age (years)	63 ± 11	59 ± 9	p = 0.22
Body Mass Index (kg/m^2)	35 ± 7	27 ± 5	p <0.001
Women	8 (42%)	9 (60%)	p = 0.49
Heart Rate (bpm)	74 ± 14	64 ± 12	p = 0.03
Systolic blood pressure (mmHg)	128 ± 22	135 ± 11	p = 0.33
Diastolic blood pressure (mmHg)	74 ± 14	71 ± 10	p = 0.41
Black	5 (26%)	0	p = 0.05
Smoker	2 (11%)	0	p = 0.50
Hypertension	16 (84%)	3 (20%)	p <0.001
Hyperlipidemia	14 (74%)	1 (7%)	p <0.001
Diabetes mellitus	11 (58%)	0	p <0.001
Brain natriuretic peptide (pg/ml)	135 ± 153	26 ± 37	p = 0.01
Hematocrit (%)	39 ± 5	44 ± 4	p = 0.007
Loop diuretic	18 (95%)	1 (7%)	p <0.001
Beta Blocker	14 (74%)	0	p <0.001
Angiotensin converting enzyme inhibitor/angiotensin receptor blocker	14 (74%)	3 (20%)	p = 0.005
Statin	14 (74%)	1 (7%)	p <0.001

Values are presented as mean ± SD or n (%).

Hyperlipidemia defined by a previous documentation of total cholesterol >200 mg/dl or low-density lipoprotein >130 mg/dl or high-density lipoprotein <40 mg/dl or current use of lipid-lowering agent.

A comparison of demographic and clinical characteristics between HFpEF and control group is summarized in Table 1. There was no significant difference in age, gender, systolic blood pressure, or history of tobacco use. Average heart rate and body mass index were significantly higher in the HFpEF group. There are notable differences in cardiovascular risk factors between the 2 groups. The HFpEF group had a significantly higher prevalence of hypertension (84%), hyperlipidemia (74%), and diabetes (58%). As expected, there were more patients in the HFpEF group taking cardiovascular medications including diuretics, β-blockers, ACE-inhibitor or ARB, and statins. Ninety-five percent of the HFpEF patients were on a loop-diuretic at the time of enrollment. Brain natriuretic peptide was elevated in HFpEF patients compared with normal controls.

Table 2 summarizes the CMR, echocardiographic, and cardiopulmonary exercise testing test results for the HFpEF and control groups. There was no between group difference in LVEF, LV mass index, or LV end-diastolic volume index. 16 HFpEF patients and all 15 controls underwent stress perfusion CMR. Of the 3 patients that did not undergo stress, 1 opted not to, and 2 had technical difficulties with perfusion. Figure 1 illustrates the perfusion maps for a patient with reduced global MPR. Global MPR was lower in the HFpEF group (2.29 ± 0.64 vs 3.38 ± 0.76, p = 0.002). Furthermore, 69% of the HFpEF group had CMD, defined as a global MPR <2.5. ECV was higher in the HFpEF group (0.29 ± 0.04 vs 0.25 ± 0.04, p = 0.02). However, native T1 was similar between groups. Six of the 19 (32%) HFpEF patients had LGE, 3 patients had subendocardial LGE in a single vessel territory, and 3 had LGE in nonischemic patterns (mid-wall and right ventricular insertion site). DENSE peak systolic circumferential strain and early diastolic circumferential strain rate were similar between groups. GLS by echo trended toward a decrease in GLS in the HFpEF group, however the study was not specifically powered to detect the difference. All 15 patients in the control group had sufficient echo quality to perform strain analysis. Only 12 (63%) of patients in the HFpEF group met appropriate image quality for performing strain analysis. The HFpEF group had a significantly higher pulmonary artery systolic (PASP) and average early mitral inflow velocity/mitral annular early diastolic velocity ratio (E/e') but similar left atrial volume index. HFpEF group had a significantly lower VO_2max and METS compared with the control group.

Correlation between MPR or ECV and different covariates are summarized in Table 3. VO_2 max was positively

Table 2
CMR, Echocardiogram, and CPET Parameters comparing heart failure with preserved ejection fraction (HFpEF) patients and controls

Variable	HFpEF (n = 19)	Controls (n = 15)	p Value
Left ventricular ejection fraction (%)	61 ± 9	65 ± 5	p = 0.13
Left ventricular mass index (g/m^2)	45 ± 12	46 ± 11	p = 0.76
Left ventricular end diastolic volume index (ml/m^2)	70 ± 14	70 ± 14	p = 0.96
Peak average circumferential strain	−0.15 ± 0.03	−0.16 ± 0.03	p = 0.60
Early diastolic circumferential strain rate	1.37 ± 0.65	1.26 ± 0.48	p = 0.59
Native T1 (ms)	1040 ± 74	1020 ± 43	p = 0.36
Partition coefficient (λ)	0.48 ± 0.05	0.45 ± 0.05	p = 0.14
Extracellular volume fraction	0.29 ± 0.04	0.25 ± 0.04	p = 0.02
Global myocardial perfusion reserve*	2.29 ± 0.64	3.38 ± 0.76	p = 0.002
Stress perfusion*	1.62 ± 0.52	1.78 ± 0.57	p = 0.43
Rest perfusion*	0.73 ± 0.23	0.54 ± 0.19	p = 0.02
Left atrium volume index (ml/m^2)	34.5 ± 15.4	26.5 ± 7.2	p = 0.09
Pulmonary artery systolic pressure (mm Hg)	35.4 ± 13.7	22.3 ± 5.4	p = 0.004
Average early mitral inflow velocity/mitral annular early diastolic velocity ratio	15.0 ± 7.6	8.6 ± 2.0	p = 0.005
Global longitudinal strain (%)	−17.9 ± 3.5	−20.5 ± 3.6	p = 0.07
Maximum oxygen consumption (ml/kg*min)	16.5 ± 6.8	30.9 ± 7.7	p <0.001
Metabolic equivalents (kcal/kg*h)	4.7 ± 1.9	8.8 ± 2.2	p <0.001

* 16/19 HFpEF patients and all control subjects underwent stress perfusion CMR. Values are presented as mean ± SD.

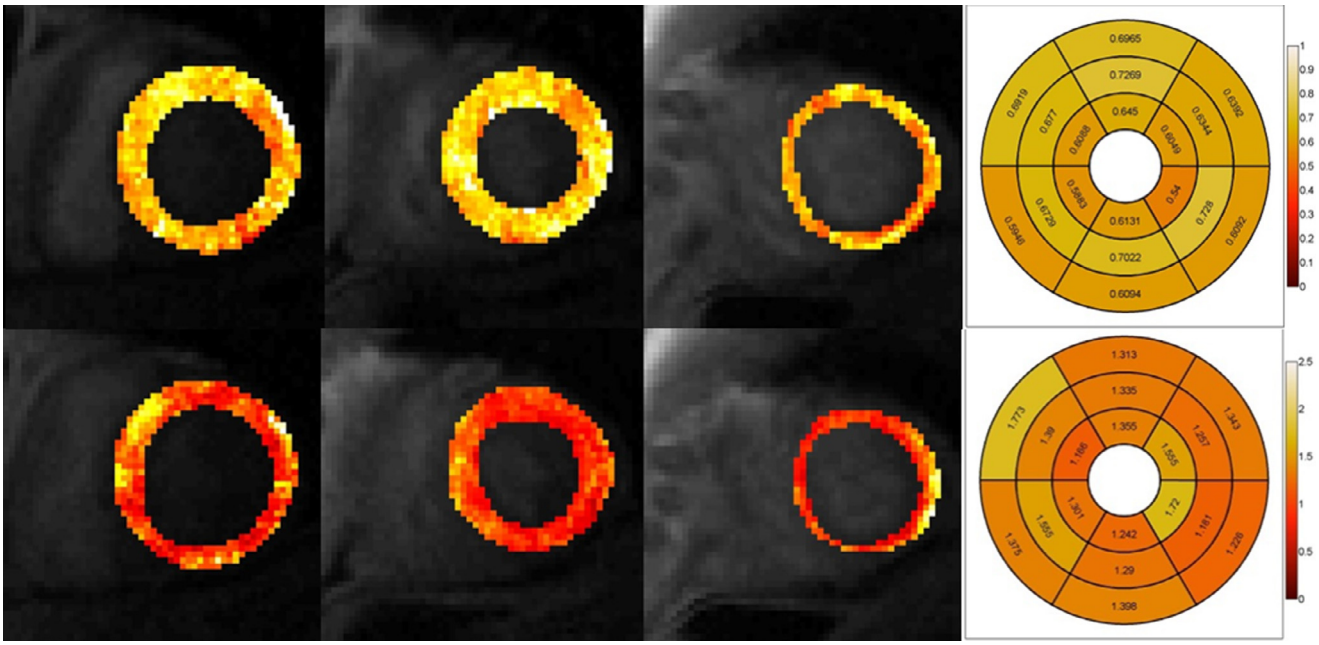

Figure 1. Pixel based perfusion maps and bulls-eye plots at rest (*top*) and stress (*bottom*) for 3 short axis slices. Global MPR for this patient was: 2.19 ± 0.31.

correlated with MPR whereas average E/e' and PASP were negative correlated. PASP had the strongest negative correlation. VO_2 max had negative correlation with ECV whereas PASP had a positive correlation. Average E/e' had no correlation with ECV. In addition, a significant negative correlation between ECV and MPR can be seen in Figure 2.

Discussion

The present study demonstrates that patients with a clinical diagnosis of HFpEF have reduced MPR and increased myocardial fibrosis as assessed by CMR compared with age-matched controls. In addition, global MPR and ECV were inversely correlated. Patients in the HFpEF cohort had significantly reduced VO_2 max, increased E/e' and PASP on echo, and elevated BNP, thus confirming their clinical HFpEF. VO_2 max, average E/e', and PASP also correlated with MPR with PASP having the highest negative correlation. The absence of Left Ventricular Hypertrophy (LVH) and known obstructive CAD underscores that the reduction in global MPR is not due to these factors. This suggests that CMD and diffuse fibrosis may play an important role in the pathophysiology of HFpEF and potentially be key targets for therapeutic interventions.

In this cohort, the prevalence of CMD, defined as global MPR <2.5,[1,29] was high (69%). This is consistent with the prevalence (75%) of CMD reported in a recent large multicenter study of coronary flow reserve assessment using adenosine stress transthoracic Doppler echocardiography in HFpEF patients.[1] This adds to the emerging literature suggesting that HFpEF is a systemic disorder associated with endothelial dysfunction.[1–7] This is the first study to assess CMD in HFpEF by CMR first pass perfusion imaging. Fully quantitative CMR has recently identified reduced MPR in patients with angina and risk factors for CMD who had no CAD.[22]

CMR has the advantage over other modalities in that it can also quantify diffuse myocardial fibrosis. ECV has been shown to be elevated in patients with LVH.[18] ECV can also

Table 3
Pearson correlation coefficients

	Pearson r	p
ECV		
VO_2max	−0.52	0.002
Average E/e'	0.34	0.057
PASP	0.51	0.006
MPR		
VO_2max	0.40	0.028
Average E/e'	−0.47	0.008
PASP	−0.60	0.001

ECV = extracelluar volume; E/e' = early mitral inflow velocity/mitral annular early diastolic velocity ratio; METS = metabolic equivalents; MPR = myocardial perfusion reserve; PASP = pulmonary artery systolic pressure; VO_2max = maximum oxygen consumption.

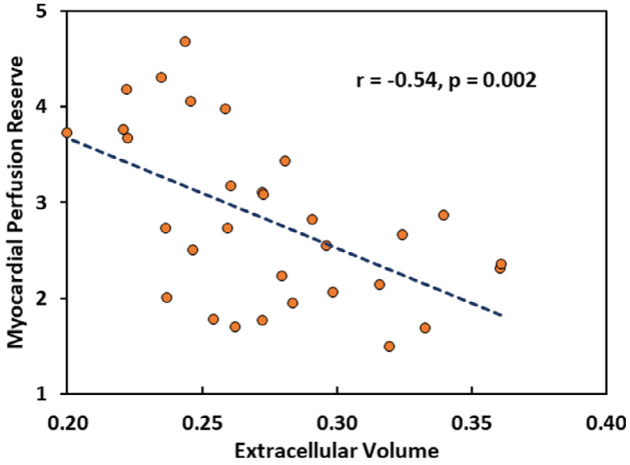

Figure 2. Scatter plot of correlation between ECV and MPR.

help differentiate HFpEF patients from hypertensive heart disease.[30] Despite our cohort demonstrating no hypertrophy, ECV was still elevated compared with the control group. Interestingly our study showed that measurements of myocardial strain, both by CMR and echocardiography, were not reduced in the HFpEF group. A recent study in patients with HFpEF, hypertensive patients, and healthy controls showed that although both GLS and ECV could discriminate between hypertensive heart disease and HFpEF, ECV was a better discriminatory marker of HFpEF (Area under the ROC Curve 0.88) than GLS (Area under the ROC Curve 0.78).[30] Their cohort had significantly less diabetics compared with the present study (9.7% vs 58%) and higher LV mass index (70.8 $\pm$ 20.2 vs 45 $\pm$ 12 g/m^2) suggesting that in a HFpEF cohort predominated by diabetic patients without LVH, increase in ECV occurs before impairment in strain. Furthermore, this study illustrates the challenge of acquiring high quality images for speckle tracking assessment of GLS in HF patients which was only achievable in <2/3 of the HFpEF cohort.

Multiple techniques have been used to assess microvascular function.[29] The advent of noninvasive techniques increases the feasibility of diagnosing CMD without the associated risk of catheter-based techniques. Doppler echocardiography techniques rely on the quality of acoustic windows and are not often used in the clinical setting. PET perfusion imaging has become a gold standard; however CMR has the added advantage of including fibrosis and strain imaging. The global MPR measured in our cohort (2.29 $\pm$ 0.64) was very similar to measurements by PET (2.16 $\pm$ 0.69) in a cohort of HFpEF patients without known obstructive CAD.[5] Future studies are needed to assess if MPR can be used to assess disease progression in HFpEF. Clinical trials targeting fibrosis and perfusion in the HFPEF population are needed.

This study is limited by a relatively small sample size; however, this pilot study is the only study to date evaluating quantitative CMR first pass perfusion imaging in HFpEF and assessing the relation between MPR and myocardial fibrosis. Furthermore, while the study was specifically powered to detect differences in MPR by CMR, it was adequately powered to highlight important differences in CMR (MPR and ECV), echocardiographic evidence of diastolic dysfunction (E/e' and PASP), and cardiopulmonary exercise testing parameters in a cohort with patients with well-characterized HFpEF with normal LV mass and LVEF.

In conclusion, we have demonstrated by quantitative CMR perfusion imaging that HFpEF patients without LVH and with normal myocardial strain, have diffuse fibrosis and a high prevalence of CMD. Comprehensive evaluation of perfusion, fibrosis, and strain by CMR may become important end points for therapeutic efficacy in HFpEF.

Disclosures

Dr. Kramer is a consult for Bayer. Drs. Salerno and Epstein receive research support from Siemens Healthineers. Dr. Salerno receives grant support from Astra Zeneca. Dr. Gan is an employee of Astra Zeneca.

Acknowledgment

The authors would like to acknowledge the help of our study coordinators and nurses Jayne Missel RN, and Caroline Flournoy PhD, our research CMR technologists Joseph Hylton, RT(R)MR and Jose Reyes RT(R)MR, and our research echo sonographers Kimberly Chadwell RDCS, Jason Higginson RDCS, and Dale E. Fowlder MD, RDCS.

1. Shah SJ, Lam CSP, Svedlund S, Saraste A, Hage C, Tan RS, Beussink-Nelson L, Fermer ML, Broberg MA, Gan LM, Lund LH. Prevalence and correlates of coronary microvascular dysfunction in heart failure with preserved ejection fraction: PROMIS-HFpEF. *Eur Heart J* 2018;39:3439–3450.
2. Paulus WJ, Tschope C. A novel paradigm for heart failure with preserved ejection fraction: comorbidities drive myocardial dysfunction and remodeling through coronary microvascular endothelial inflammation. *J Am Coll Cardiol* 2013;62:263–271.
3. Sucato V, Evola S, Novo G, Sansone A, Quagliana A, Andolina G, Assennato P, Novo S. Angiographic evaluation of coronary microvascular dysfunction in patients with heart failure and preserved ejection fraction. *Microcirculation* 2015;22:528–533.
4. Dryer K, Gajjar M, Narang N, Lee M, Paul J, Shah AP, Nathan S, Butler J, Davidson CJ, Fearon WF, Shah SJ, Blair JEA. Coronary microvascular dysfunction in patients with heart failure with preserved ejection fraction. *Am J Physiol Heart Circ Physiol* 2018;314:H1033–H1042.
5. Srivaratharajah K, Coutinho T, deKemp R, Liu P, Haddad H, Stadnick E, Davies RA, Chih S, Dwivedi G, Guo A, Wells GA, Bernick J, Beanlands R, Mielniczuk LM. Reduced myocardial flow in heart failure patients with preserved ejection fraction. *Circ Heart Fail* 2016;9:e002562.
6. Kato S, Saito N, Kirigaya H, Gyotoku D, Iinuma N, Kusakawa Y, Iguchi K, Nakachi T, Fukui K, Futaki M, Iwasawa T, Kimura K, Umemura S. Impairment of coronary flow reserve evaluated by phase contrast cine-magnetic resonance imaging in patients with heart failure with preserved ejection fraction. *J Am Heart Assoc* 2016;5:e002649.
7. Mohammed SF, Hussain S, Mirzoyev SA, Edwards WD, Maleszewski JJ, Redfield MM. Coronary microvascular rarefaction and myocardial fibrosis in heart failure with preserved ejection fraction. *Circulation* 2015;131:550–559.
8. Lockie T, Ishida M, Perera D, Chiribiri A, De Silva K, Kozerke S, Marber M, Nagel E, Rezavi R, Redwood S, Plein S. High-resolution magnetic resonance myocardial perfusion imaging at 3.0-Tesla to detect hemodynamically significant coronary stenoses as determined by fractional flow reserve. *J Am Coll Cardiol* 2011;57:70–75.
9. Morton G, Chiribiri A, Ishida M, Hussain ST, Schuster A, Indermuehle A, Perera D, Knuuti J, Baker S, Hedstrom E, Schleyer P, O'Doherty M, Barrington S, Nagel E. Quantification of absolute myocardial perfusion in patients with coronary artery disease: comparison between cardiovascular magnetic resonance and positron emission tomography. *J Am Coll Cardiol* 2012;60:1546–1555.
10. Zile MR, Brutsaert DL. New concepts in diastolic dysfunction and diastolic heart failure: Part I: diagnosis, prognosis, and measurements of diastolic function. *Circulation* 2002;105:1387–1393.
11. Iles L, Pfluger H, Phrommintikul A, Cherayath J, Aksit P, Gupta SN, Kaye DM, Taylor AJ. Evaluation of diffuse myocardial fibrosis in heart failure with cardiac magnetic resonance contrast-enhanced T1 mapping. *J Am Coll Cardiol* 2008;52:1574–1580.
12. Flett AS, Hayward MP, Ashworth MT, Hansen MS, Taylor AM, Elliott PM, McGregor C, Moon JC. Equilibrium contrast cardiovascular magnetic resonance for the measurement of diffuse myocardial fibrosis: preliminary validation in humans. *Circulation* 2010;122:138–144.
13. Duca F, Kammerlander AA, Zotter-Tufaro C, Aschauer S, Schwaiger ML, Marzluf BA, Bonderman D, Mascherbauer J. Interstitial Fibrosis, functional status, and outcomes in heart failure with preserved ejection fraction: insights from a prospective cardiac magnetic resonance imaging study. *Circ Cardiovasc Imaging* 2016;9:e005277.
14. Salerno M, Kramer CM. Myocardial extracellular volume: unifying form and function in heart failure with preserved ejection fraction. *J Am Coll Cardiol* 2016;67:1826–1828.
15. Salerno M. Seeing the unseen fibrosis in heart failure with preserved ejection fraction. *JACC Cardiovasc Imaging* 2014;7:998–1000.

16. Kim D, Gilson WD, Kramer CM, Epstein FH. Myocardial tissue tracking with two-dimensional cine displacement-encoded MR imaging: development and initial evaluation. *Radiology* 2004;230:862–871.
17. Zhong X, Spottiswoode BS, Meyer CH, Kramer CM, Epstein FH. Imaging three-dimensional myocardial mechanics using navigator-gated volumetric spiral cine DENSE MRI. *Magn Reson Med* 2010;64:1089–1097.
18. Kuruvilla S, Janardhanan R, Antkowiak P, Keeley EC, Adenaw N, Brooks J, Epstein FH, Kramer CM, Salerno M. Increased extracellular volume and altered mechanics are associated with LVH in hypertensive heart disease, not hypertension alone. *JACC Cardiovasc Imaging* 2015;8:172–180.
19. Hsu LY, Jacobs M, Benovoy M, Ta AD, Conn HM, Winkler S, Greve AM, Chen MY, Shanbhag SM, Bandettini WP, Arai AE. Diagnostic performance of fully automated pixel-wise quantitative myocardial perfusion imaging by cardiovascular magnetic resonance. *JACC Cardiovasc Imaging* 2018;11:697–707.
20. Cernicanu A, Axel L. Theory-based signal calibration with single-point T1 measurements for first-pass quantitative perfusion MRI studies. *Acad Radiol* 2006;13:686–693.
21. Kramer CM, Barkhausen J, Flamm SD, Kim RJ, Nagel E. Society for cardiovascular magnetic resonance board of trustees task force on standardized protocols. Standardized cardiovascular magnetic resonance (CMR) protocols 2013 update. *J Cardiovasc Magn Reson* 2013;15. 91-429X-15-91.
22. Zorach B, Shaw PW, Bourque J, Kuruvilla S, Balfour PC Jr, Yang Y, Mathew R, Pan J, Gonzalez JA, Taylor AM, Meyer CH, Epstein FH, Kramer CM, Salerno M. Quantitative cardiovascular magnetic resonance perfusion imaging identifies reduced flow reserve in microvascular coronary artery disease. *J Cardiovasc Magn Reson* 2018;20:14.. 018-0435-1.
23. Kellman P, Wilson JR, Xue H, Ugander M, Arai AE. Extracellular volume fraction mapping in the myocardium, part 1: evaluation of an automated method. *J Cardiovasc Magn Reson* 2012;14. 63-429X-14-63.
24. Salerno M, Kramer CM. Advances in parametric mapping with CMR imaging. *JACC Cardiovasc Imaging* 2013;6:806–822.
25. Spottiswoode BS, Zhong X, Lorenz CH, Mayosi BM, Meintjes EM, Epstein FH. Motion-guided segmentation for cine DENSE MRI. *Med Image Anal* 2009;13:105–115.
26. Spottiswoode BS, Zhong X, Hess AT, Kramer CM, Meintjes EM, Mayosi BM, Epstein FH. Tracking myocardial motion from cine DENSE images using spatiotemporal phase unwrapping and temporal fitting. *IEEE Trans Med Imaging* 2007;26:15–30.
27. Lang RM, Badano LP, Mor-Avi V, Afilalo J, Armstrong A, Ernande L, Flachskampf FA, Foster E, Goldstein SA, Kuznetsova T, Lancellotti P, Muraru D, Picard MH, Rietzschel ER, Rudski L, Spencer KT, Tsang W, Voigt JU. Recommendations for cardiac chamber quantification by echocardiography in adults: an update from the American Society of Echocardiography and the European Association of Cardiovascular Imaging. *J Am Soc Echocardiogr* 2015;28:1–39. e14.
28. Nagueh SF, Smiseth OA, Appleton CP, Byrd BF 3rd, Dokainish H, Edvardsen T, Flachskampf FA, Gillebert TC, Klein AL, Lancellotti P, Marino P, Oh JK, Popescu BA, Waggoner AD. Recommendations for the evaluation of left ventricular diastolic function by echocardiography: an update from the American Society of Echocardiography and the European Association of Cardiovascular Imaging. *J Am Soc Echocardiogr* 2016;29:277–314.
29. Marinescu MA, Loffler AI, Ouellette M, Smith L, Kramer CM, Bourque JM. Coronary microvascular dysfunction, microvascular angina, and treatment strategies. *JACC Cardiovasc Imaging* 2015;8:210–220.
30. Mordi IR, Singh S, Rudd A, Srinivasan J, Frenneaux M, Tzemos N, Dawson DK. Comprehensive echocardiographic and cardiac magnetic resonance evaluation differentiates among heart failure with preserved ejection fraction patients, hypertensive patients, and healthy control subjects. *JACC Cardiovasc Imaging* 2018;11:577–585.